ORIGINAL ARTICLE

Prospective Study

Multimodality functional imaging using DW-MRI and 18F-FDG-PET/CT during radiation therapy for human papillomavirus negative head and neck squamous cell carcinoma: Meixoeiro Hospital of Vigo Experience

David Aramburu Núñez, Antonio Lopez Medina, Moisés Mera Iglesias, Francisco Salvador Gomez, Abhay Dave, Vaios Hatzoglou, Ramesh Paudyal, Alfonso Calzado, Joseph O Deasy, Amita Shukla-Dave, Victor M Muñoz

David Aramburu Núñez, Antonio Lopez Medina, Francisco Salvador Gomez, Department of Medical Physics and Radiological Protection, Galaria - Meixoeiro, University Hospital Complex of Vigo, 36200 Vigo, Spain

David Aramburu Núñez, Abhay Dave, Ramesh Paudyal, Joseph O Deasy, Amita Shukla-Dave, Department of Medical Physics, Memorial Sloan-Kettering Cancer Center, New York, NY 10065, United States

David Aramburu Núñez, Alfonso Calzado, Department of Radiology, Complutense University, 28040 Madrid, Spain

Moisés Mera Iglesias, Department of Medical Physics, Oncoserv, Santiago de los Caballeros 51000, Dominican Republic

Vaios Hatzoglou, Amita Shukla-Dave, Department of Radiology, Memorial Sloan-Kettering Cancer Center, New York, NY 10065, United States

Victor M Muñoz, Department of Radiation Oncology, Galaria - Meixoeiro, University Hospital Complex of Vigo, 36200 Vigo, Spain

Correspondence to: Amita Shukla-Dave, PhD, Director Quantitative Imaging, Department of Medical Physics, Memorial Sloan-Kettering Cancer Center, 1275 York Avenue, New York, NY 10065, United States. davea@mskcc.org

Telephone: +1-212-6393184
Fax: +1-212-7173010

Abstract

AIM

To noninvasively investigate tumor cellularity measured using diffusion-weighted magnetic resonance imaging (DW-MRI) and glucose metabolism measured by ^{18}F-labeled fluorodeoxyglucose positron emission tomography/computed tomography (^{18}F-FDG-PET/CT) during radiation therapy (RT) for human papillomavirus negative (HPV-) head and neck squamous cell carcinoma (HNSCC).

METHODS

In this prospective study, 6 HPV- HNSCC patients underwent a total of 34 multimodality imaging examinations (DW-MRI at 1.5 T Philips MRI scanner [(n = 24) pre-, during- (2-3 wk), and post-treatment (Tx), and ^{18}F-FDG PET/CT pre- and post-Tx (n = 10)]. All patients received RT. Monoexponential modeling of the DW-MRI data yielded the imaging metric apparent diffusion coefficient (ADC) and the mean of standardized uptake value (SUV) was measured from ^{18}F-FDG PET uptake. All patients had a clinical follow-up as the standard of care and survival status was documented at 1 year.

RESULTS

There was a strong negative correlation between the mean of pretreatment ADC (ρ = -0.67, P = 0.01) and the pretreatment ^{18}F-FDG PET SUV. The percentage (%) change in delta (Δ) ADC for primary tumors and neck nodal metastases between pre- and Wk2-3 Tx were as follows: 75.4% and 61.6%, respectively, for the patient with no evidence of disease, 27.5% and 32.7%, respectively, for those patients who were alive with disease, and 26.9% and 7.31%, respectively, for those who were dead with disease.

CONCLUSION

These results are preliminary in nature and are indicative, and not definitive, trends rendered by the imaging metrics due to the small sample size of HPV- HNSCC patients in a Meixoeiro Hospital of Vigo Experience.

Key words: Diffusion-weighted magnetic resonance imaging; Human papillomavirus negative head and neck squamous cell carcinoma; ^{18}F-labeled fluorodeoxyglucose positron emission tomography/computed tomography

Core tip: In the modern era of adaptive radiotherapy, it is crucial to understand how different imaging techniques interact and complement each other for application in cancer care. The quantitative imaging metrics, apparent diffusion coefficient and standardized uptake value, play a significant role in understanding the efficacy of the radiotherapy treatment. Tumor cellularity and glucose metabolism were investigated before, during, and after radiotherapy in human papillomavirus negative head and neck squamous cell carcinoma patients using the diffusion-weighted magnetic resonance imaging and ^{18}F-labeled fluorodeoxyglucose positron emission tomography/computed tomography imaging techniques.

INTRODUCTION

The Spanish Cancer Registries reported that in 2014, 241284 new cases of cancer were diagnosed in Spain[1]. Out of these, 12696 were head and neck (HN) cancers in which approximately 90% were specifically squamous cell carcinomas (SCC)[2]. The main subgroup for the patients was oropharyngeal SCC wherein 52%-72% of the cases were caused by infection from the human papillomavirus (HPV)[3]. It has been previously reported that HPV negative (-) HNSCC patients have poor outcomes compared with HPV-positive (HPV+) cancers[4]. Thus, in an effort to perform biologically guided adaptive radiotherapy, it is critical to understand how different functional imaging techniques interact and potentially complement each other[5]. Multimodality imaging, such as diffusion-weighted magnetic resonance imaging (DW-MRI) and ^{18}F-labeled fluorodeoxyglucose positron emission tomography/computed tomography (^{18}F-FDG-PET/CT), can provide useful anatomical and functional quantitative imaging metrics.

DW-MRI provides a noninvasive measurement for the degree of random motion of water in tissue; the rate of this diffusion is quantified by a quantitative imaging metric, the apparent diffusion coefficient (ADC)[6]. The advantage of DW-MRI over traditional anatomical MRI is that it can reflect the tissue cellularity and the integrity of cell membranes[7]. A recent metaanalysis reported that ADC has an inverse correlation with tissue cell density[8]. Kim *et al*[9] have shown that a significant increase in ADC was observed within 1 wk of treatment in HNSCC patients who were complete responders (P < 0.01). The Vandecaveye
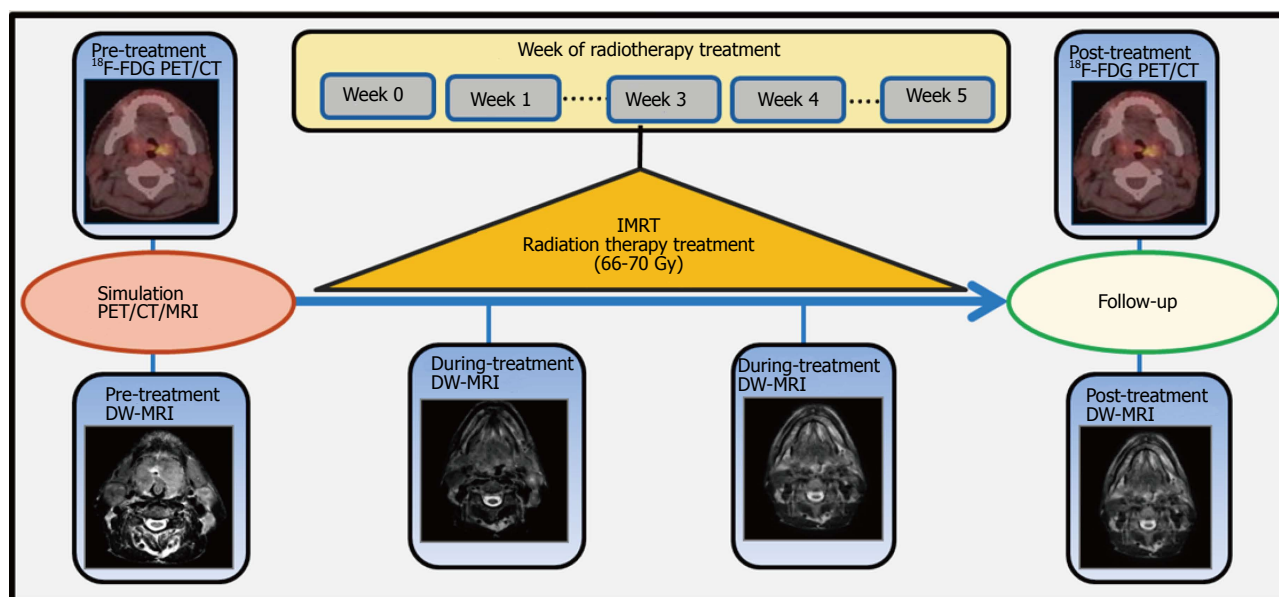
Figure 1 Workflow representing the study design performed in all the patients. ^{18}F-FDG: Fluorine-18 Fludeoxyglucose; PET/CT: Positron emission tomography/computed tomography; DW-MRI: Diffusion-weighted magnetic resonance imaging.

et al[10] study further established the utility of ADC in differentiating responding from non-responding HNSCC by providing a threshold (25% and 20% for primary tumors and lymph node metastases, respectively) for the percent relative (Δ) ADC change between pre-treatment (Tx) and 3 wk post-chemoradiotherapy (post-CRT).

Another quantitative imaging metric, standardized uptake value (SUV), obtained from ^{18}F-FDG PET is a measure of glucose metabolism. An abnormally elevated SUV can be observed in most primary and metastatic cancers including HNSCC[11]. The ^{18}F-FDG PET/CT has an established role in HNSCC management, including staging and monitoring CRT response[12,13]. The Schwartz *et al*[14] study showed that primary tumor SUV was a promising prognostic factor in HNSCC patients.

A better understanding of the association between ^{18}F-FDG PET/CT and DW-MRI derived quantitative imaging metrics is needed in order for them to become the building blocks for a biologically-guided adaptive radiotherapy. Recently there have been few reports showing correlations between these multimodality imaging techniques and their initial role in the prognosis of HNSCC patients[15]. However, there are limited studies initiated to explore the use of these techniques together in a treatment planning setting for radiation oncology[16]. Our study is the first experience in Spain with multimodality imaging in HPV-HNSCC patients for its use in biologically-guided adaptive radiotherapy. The purpose of the current study is to non-invasively investigate tumor cellularity measured using DW-MRI and glucose metabolism measured by ^{18}F-FDG-PET/CT during RT for HPV- HNSCC.

MATERIALS AND METHODS

Patients
This prospective study was conducted in accordance with the Declaration of Helsinki[17]. The study protocol was approved by the local ethics committee; informed consent was obtained from all patients. All patients eligible for this study had biopsy-proven newly diagnosed squamous cell carcinoma of the head and neck. Diagnostic biopsies were also performed to evaluate HPV status. Six HPV- HNSCC patients underwent a total of 34 multimodality imaging examinations [DW-MRI at 1.5 T Philips MRI scanner (n = 24) pre-, during (2-3 wk) and post-Tx, and ^{18}F-FDG PET/CT pre- and post-Tx (n = 10)] (Figure 1). All the patients were treated with intensity-modulated radiation therapy (IMRT), and the prescribed doses varied between 66 Gy and 70 Gy to the local planning target volume (PTV). Patient characteristics are given in Table 1.

All the patients had a clinical follow-up as the standard of care and survival status was documented into groups at 1 year. The four groups for patients were as follows: No evidence of disease (NED), alive with disease (AWD), dead of disease (DOD), and dead of other causes (DOC). Additionally, local-regional and distant metastases statuses were noted for all patients[18].

DWI-MRI
All MRI examinations were performed on a 1.5-Tesla Achieva scanner (Philips Healthcare, The Netherlands) with a Philips Sense Flex coil over the neck. For MRI, all patients were in the supine position with an immobilization system that was also used during the radiotherapy treatment delivery. A thermoplastic mask, head support, and flat table were used to minimize distortion and improve the registration process between the different imaging modalities. The head support and flat table were adapted to the MRI/safety requirements. The MRI protocol consisted of the standard anatomic MRI scans (T1-/T2-weighted images) and DW-MRI.

DW-MRI acquisition was performed using single-shot echo planar imaging (SS-EPI) with three b values (b =

Table 1 Characteristics of the patients involved in this study

Characteristics	Value
Demographics	
Mean age (yr)	65
Age range (yr)	52-79
Male/female	5/1
Location of primary tumor	
Oropharynx	6
Metastatic loco-regional nodes	11
Radiation therapy technique	IMRT
Dose (Gy)	66-70
Fractions	32
Outcome	
Alive with disease	3
Dead of disease	2
No evidence of disease	1

0, 600 and 1000 s/mm^2). Other parameters included repetition time (TR) = 5000 ms, echo time (TE) = 77-100 ms, number of excitations (NEX) = 2, field of view (FOV): 24 cm, and slice thickness = 6 mm. The total acquisition time for obtaining the DW-MRI data was approximately 5 min. The acquisition matrix of 120 × 97 was zero filled to 256 × 256 during image reconstruction.

^{18}F-FDG PET/CT

A whole-body PET/CT scan was performed from head to thigh, 60 min after intravenous administration of approximately 370 MBq (± 10%) of ^{18}F-FDG on a PET/CT Discovery scanner (GE Healthcare Bio-Sciences Corp.). The patient was placed in the supine position, with the same immobilization system as in the radiotherapy treatment delivery. Other parameters included a 70 cm axial FOV, a 218 × 218 matrix. Data was acquired in a 3-D mode. The pixel spacing was 5.47 mm with a slice thickness of 3.27 mm. The spatial resolution varied from 3.99 mm to 4.56 mm. PET images were corrected using the specific software of the equipment for attenuation, scatter, decay, dead time, random coincidences, and slice sensitivity.

Image analysis

All images were registered and analyzed using in-house software (Artfibio-tool)[19]. The registration for DW-MRI and ^{18}F-FDG PET/CT datasets was a two-step process: (1) Manual registration: performing a manual alignment (translation and/or rotation) of the images (DWMRI, CT-Scan, PET-CT) interactively on-screen; and (2) Automatic Rigid Registration: Once the images were approximately aligned, a more precise alignment (full rigid transformation) was performed based on an iterative process evaluated by statistical metrics (Viola and Wells mutual information[20]). Using Artfibio-tool, the signal intensity values were extracted from the whole tumor volumes[19].

DW-MRI: According to Stejskal and Tanner's[21] and considering the monoexponential approximation (7), the ADC value was calculated using equation 1:

$$ADC = [\log_e(s_0/s_1)]/(b_1 - b_0). \quad (1)$$

Where S_1 and S_0 are signal values of the images at b values, b_1 and b_0, respectively, and ADC is the apparent diffusion coefficient.

Regions of Interest (ROIs) were delineated on the primary tumor and neck nodal metastases by an experienced neuroradiologist on the DW-MRI image (b = 0 s/mm^2). Before contouring the ROIs, the T1-T2-weighted images were used to determine localization and tumor extent.

Finally, a relative percentage (%) change in derived imaging metric (ADC) between pre- and i^{th} intra-Tx week (Wk) was calculated as follows:

$$\Delta ADC\,(\%) = [(ADC_i - ADC_0)/ADC_0] \times 100. \quad (2)$$

Where i^{th} represents intra-TX week for ADC metric value and ADC_0 represents the pre-Tx metric value.

^{18}F-FDG PET/CT: An experienced radiation oncologist matched the ROIs from the MR images with those of the PET/CT images and analyzed them qualitatively and quantitatively using the attenuation-corrected PET emission images. The ROIs were placed over the areas of focal ^{18}F-FDG uptake in both the primary tumor and neck nodal metastases. The intensity of the ^{18}F-FDG uptake in the ROIs was measured using the SUV normalized by the dilution volume[22]. The imaging data available in units of mCi per mL (mCi/mL) per voxel were decay-corrected to the time of injection and converted to SUV units.

Statistical analysis

In the present study, data was analyzed from a total of 34 multimodality imaging studies [DW-MRI (*n* = 24) pre-, during- (2-3 wk) and post-Tx and ^{18}F-FDG PET/CT pre- and post-Tx (*n* = 10)] to capture treatment response. Values were presented as mean ± SD. The mean value comparison was carried out using the Wilcoxon test. A Spearman correlation analysis was performed between SUV and ADC metric values, which we used to report the correlation and *P*-values. These correlations were reported using the standard guidelines[23] in which an absolute correlation of < 0.3 was considered weak, 0.3-0.5 was considered moderate and 0.5-1.0 was considered strong. The significance level was set at $P \leqslant 0.05$. All data analysis was performed using the R software/environment, an open source project that is distributed under the GNU General Public License[24].

RESULTS

All 6 patients were untreated at the first time point of multimodality imaging, had biopsy-proven SCC, and were HPV-. Among the 6 patients, a total of 11 neck nodal metastases and 5 primary tumors were analyzed (3 patients had more than one node and 1 patient had an unknown primary tumor site). Patients were grouped as follows based on clinical outcome: NED = 1, AWD = 3, and DOD = 2 (Table 1). A total of 34 multimodality imaging studies [DW-MRI (*n* = 24) and ^{18}F-FDG PET/
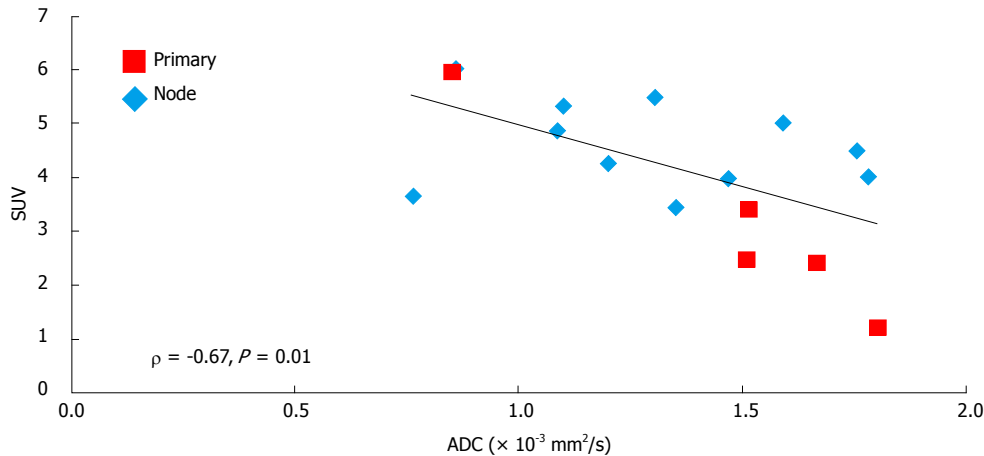
Figure 2 Relationship between pre-Tx mean standardized uptake value and pre-Tx mean apparent diffusion coefficient showing a significant strong negative inverse correlation. SUV: Standardized uptake value; ADC: Apparent diffusion coefficient.

Table 2 Apparent diffusion coefficient metric values for human papillomavirus negative head and neck squamous cell carcinoma patients who were classified based on survival as dead of disease, alive with disease and no evidence of disease before, during and post- radiotherapy

MRI	DOD ADC mean ($\times 10^{-3}$ mm^2/s)		AWD ADC mean ($\times 10^{-3}$ mm^2/s)		NED ADC mean ($\times 10^{-3}$ mm^2/s)	
	Primary	Node	Primary	Node	Primary	Node
Pre-Tx	1.51 ± 0.36	1.43 ± 0.58	1.66 ± 0.41	1.26 ± 0.19	0.85 ± 0.27	0.86 ± 0.20
During Tx (2-3 wk)	1.92 ± 0.33	1.54 ± 0.11	2.12 ± 0.38	1.41 ± 0.38	1.49 ± 0.13	1.39 ± 0.08
Post-Tx	No primary	0.98 ± 0.29	No primary	1.93 ± 0.22	No primary	No node

MRI: Magnetic resonance imaging; ADC: Apparent diffusion coefficient; AWD: Alive with disease; DOC: Dead of other causes; DOD: Dead of disease; NED: No evidence of disease.

CT (n = 10)] were analyzed to capture RT response. The results showed a significantly strong negative correlation (ρ = -0.67, P = 0.01) between the pre-Tx mean SUV and the pre-Tx mean ADC for the 11 lymph nodes and 5 primary tumors (Figure 2).

A summary of the ADC mean for pre-Tx and during-Tx (2nd and 3rd weeks data were combined) from the three different survival groups as DOD, AWD and NED is shown in Table 2. For a single patient who was NED at the last clinical follow-up, the MRI and the ^{18}F-FDG PET/CT post-treatment showed no evidence of disease at the primary tumor site and neck nodal metastases. Figure 3 shows the DW-MRI and ^{18}F-FDG PET/CT images from a patient who was NED. The ADC values (mean ± SD) for the ROI drawn on the primary tumor were 0.85 ± 0.27 × 10^{-3} mm^2/s, 1.49 ± 0.13 × 10^{-3} mm^2/s for pre-Tx and Wk$_{2-3}$ Tx, respectively. The ADC values for the ROIs in neck nodal metastases were as follows 0.86 ± 0.20 × 10^{-3} mm^2/s, 1.39 ± 0.08 × 10^{-3} mm^2/s for pre-Tx and Wk$_{2-3}$ Tx (Table 2). Pre-Tx SUV (mean ± SD) values for primary tumor and neck nodal metastases were 5.99 ± 0.61 and 6.06 ± 0.49, respectively.

Three patients were AWD on the last clinical follow-up, and 1 patient had an unknown primary tumor site. Both, MRI and ^{18}F-FDG PET/CT post-treatment showed no evidence of disease at the primary tumor site; however the neck nodal metastases were still present.

Figure 4 shows the DW-MRI and ^{18}F-FDG PET/CT images from a patient who was AWD. The ADC values (mean ± SD) for the primary tumors were 1.66 ± 0.41 × 10^{-3} mm^2/s, 2.12 ± 0.38 × 10^{-3} mm^2/s for pre-Tx and Wk$_{2-3}$ Tx, respectively. The ADC values for the neck nodal metastases were 1.26 ± 0.19 × 10^{-3} mm^2/s, 1.41 ± 0.38 × 10^{-3} mm^2/s, and 1.93 ± 0.22 × 10^{-3} mm^2/s for pre-Tx, Wk$_{2-3}$ Tx and post-Tx, respectively (Table 2). The SUV mean pre-Tx values for the primary tumor and neck nodal metastases were 1.84 ± 0.83 and 4.85 ± 0.75, respectively.

The two patients who were DOD died 2 mo and 6 mo post-Tx. Figure 5 shows the DW-MRI and ^{18}F-FDG PET/CT images from a patient who was DOD. The ADC values (mean ± SD) for the primary tumor were 1.51 ± 0.36 × 10^{-3} mm^2/s and 1.92 ± 0.33 × 10^{-3} mm^2/s for pre-Tx and Wk$_{2-3}$ Tx, respectively. The ADC values for the neck nodal metastases were 1.43 ± 0.58 × 10^{-3} mm^2/s, 1.54 ± 0.11 × 10^{-3} mm^2/s, and 0.98 ± 0.29 × 10^{-3} mm^2/s for pre-Tx, Wk$_{2-3}$ Tx and post-Tx, respectively (Table 2). The SUV mean pre-Tx values for the primary tumor and neck nodal metastases were 2.98 ± 0.66 and 3.93 ± 0.45, respectively.

The ΔADC (%) between pre- and Wk$_{2-3}$ Tx for primary tumors and neck nodal metastases were as follows: 75.4% and 61.6%, respectively, for the patient with NED, 27.5% and 32.7%, respectively, for those
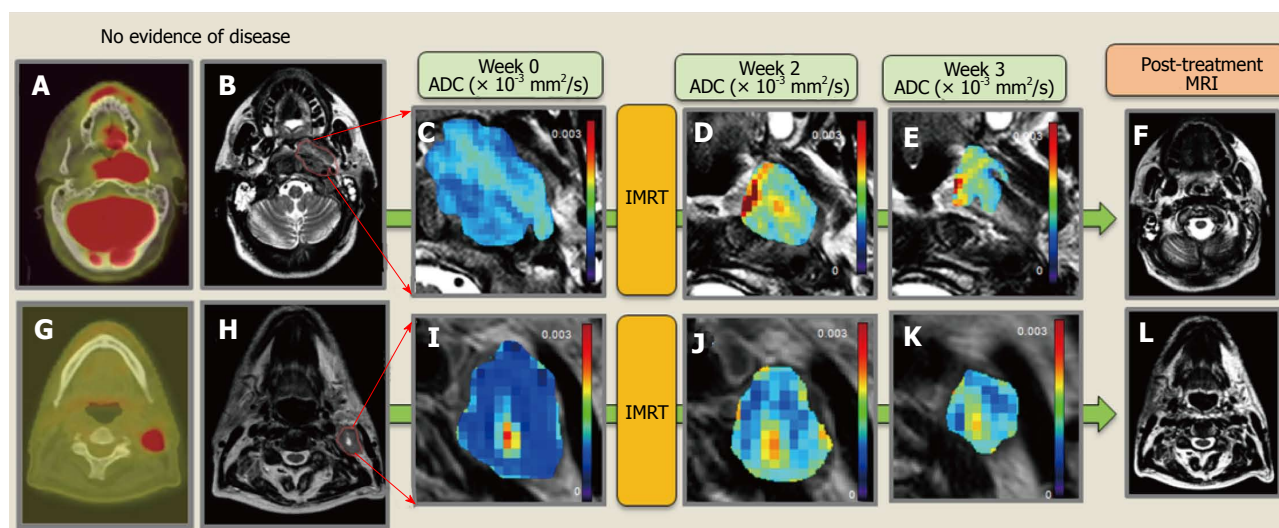
Figure 3 Representative no evidence of disease patient. A and G: Pre-Tx PET/CT of the primary tumor and a neck nodal metastasis; B and H: Primary tumor and representative neck nodal metastasis contoured over a T2-W MRI; C and I: Pre-Tx ADC map overlaid on T2-W MRI; D and J: Wk2-Tx ADC map overlaid on T2-W; E and K: Wk3-Tx ADC map overlaid on T2-W; F and L: T2-W MRI post-Tx with no evidence of primary tumor and neck nodal metastases. PET/CT: Positron emission tomography/computed tomography; MRI: Magnetic resonance imaging; ADC: Apparent diffusion coefficient; IMRT: Intensity modulated radiation therapy.
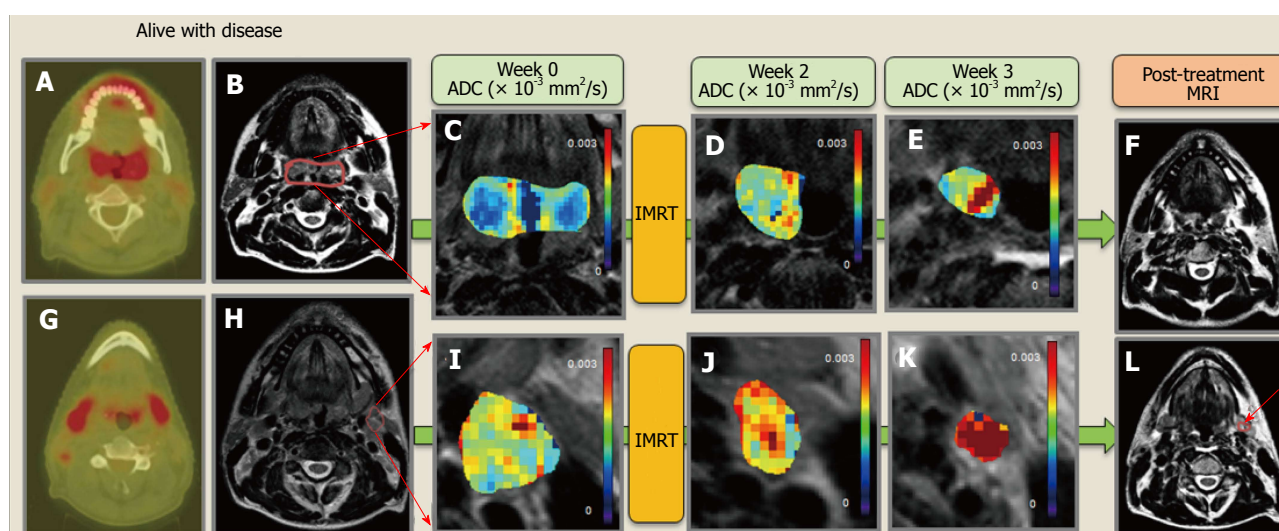
Figure 4 Representative alive with disease patient. A and G: pre-Tx PET/CT of the primary tumor and two neck nodal metastases; B and H: Primary tumor and representative neck nodal metastasis contoured over a T2-W MRI; C and I: Pre-Tx ADC map overlaid on T2-W MRI; D and J: Wk2-Tx ADC map overlaid on T2-W; E and K: Wk3-Tx ADC map overlaid on T2-W; F and L: T2-W MRI post-Tx with no evidence of primary tumor but with presence of neck nodal metastasis. PET/CT: Positron emission tomography/computed tomography; MRI: Magnetic resonance imaging; ADC: Apparent diffusion coefficient; IMRT: Intensity modulated radiation therapy.

patients who were AWD, and 26.9% and 7.31%, respectively, for those who were DOD.

DISCUSSION

This prospective study is the first in Spain conducted in support of integrating functional imaging in a RT setting. We evaluated multimodality imaging in HPV-HNSCC patients for both primary and neck nodal metastases. Specifically, we observed that pretreatment tumor cellularity is inversely proportional to glucose metabolism in these tumors, which was consistent with the previous literature[15,25,26]. The survival status and

functional metrics show different % change in ΔADC for the NED, AWD, and DOD survival groups, which would need to be validated in larger patient population studies.

HNSCC is one of the major types of cancer that can be linked to alcohol consumption and tobacco smoking. It typically originates from the mucosal epithelia of the oral cavity, pharynx and larynx[27]. In oropharyngeal SCC, HPV status is an independent prognostic factor for both overall survival and progression-free survival, which is consistent with the hypothesis that HPV+ and HPV- tumors are distinct and have different causes, risk-factor profiles, and survival outcomes[28]. HPV- tumors continue to have poor outcomes compared to
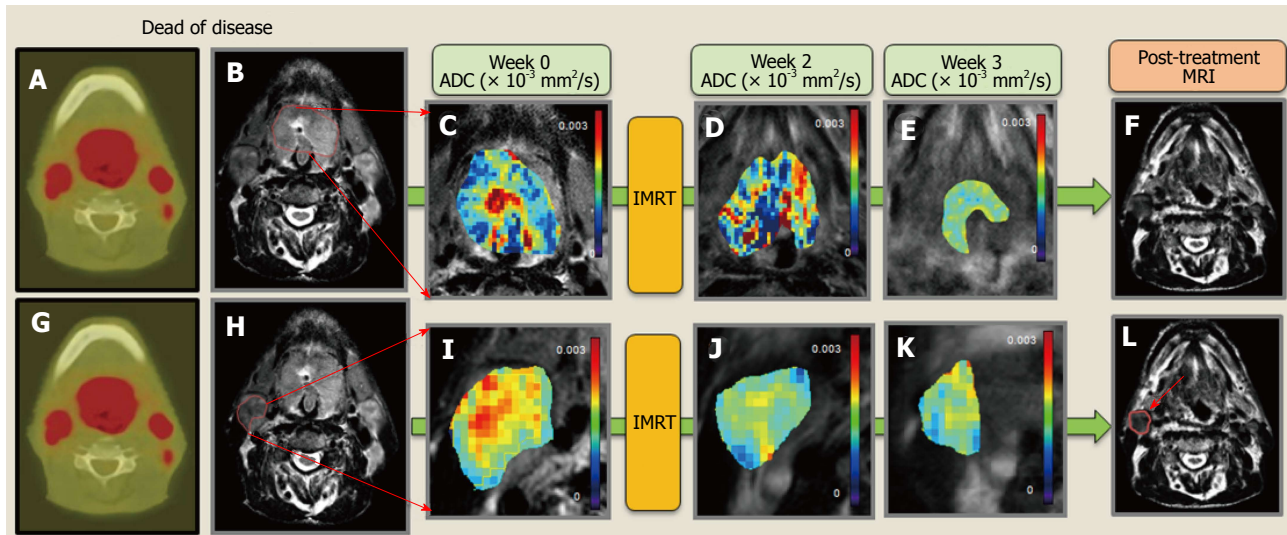
Figure 5 Representative dead of disease patient. A and G: Pre-Tx PET/CT of the primary tumor and three neck nodal metastases; B and H: Primary tumor and representative neck nodal metastasis contoured over a T2-W MRI; C and I: Pre-Tx ADC map overlaid on T2-W MRI; D and J: Wk2-Tx ADC map overlaid on T2-W; E and K: Wk3-Tx ADC map overlaid on T2-W; F and L: T2-W MRI post-Tx with no evidence of primary tumor but with presence of neck nodal metastasis. PET/CT: Positron emission tomography/computed tomography; MRI: Magnetic resonance imaging; ADC: Apparent diffusion coefficient; IMRT: Intensity modulated radiation therapy.

their HPV+ counterparts[28]. Future clinical trials should be designed specifically for patients with HPV+ or HPV- HNSCC using appropriate, validated quantitative imaging biomarkers. As there is very scarce imaging literature on HPV+ or HPV- alone, it raises an urgent need to study these cohorts independently and assess the value of multimodality imaging for better cancer patient management.

In recent years, studies by Razek have shown that ADC metric has a prognostic value in HNSCC[29-31]. They reported a mean ADC value in nasopharyngeal carcinoma (NPC) of $0.99 \pm 0.11 \times 10^{-3}$ mm^2/s. The ADC value in this study also correlated inversely with tumor volume[29]. In a separate study by the same group, it was reported that the mean ADC value of residual or recurrent lesions ($1.17 \pm 0.33 \times 10^{-3}$ mm^2/s) was less than that observed in post-therapeutic changes ($2.07 \pm 0.25 \times 10^{-3}$ mm^2/s)[30]. They also showed that ADC values with metabolic ratio (Ch/Cr) obtained from 1H-MRS are well correlated with several prognostic parameters of HNSCC[31].

The use of multimodality imaging (^{18}F-FDG PET/CT, DW-MRI, DCE-MRI) in general HNSCC populations for assessing both the association between the quantitative imaging biomarkers obtained from each imaging technique and their combined or respective roles in prognosis and/or prediction of outcome[8,25,32,33]. The major technical challenges in IMRT persist in the use of functional images for treatment, one of which includes the identification of a reproducible, RT-compatible patient positioning setup that is consistent between functional techniques and RT. All patients in the present study were in a supine position and fixed in place with the same immobilization system that was used during the RT treatment planning and delivery. A thermoplastic mask, head support, and flat table were used to try to minimize distortion and to improve the registration process between the different imaging modalities. The head support and flat table were adapted to MRI and PET/CT. This reproducible positioning addressed one of the big hurdles in the acquisition of multimodality images that may be used for adaptive RT in the future[34,35]. Dirix *et al*[36] designed a feasibility, prospective, multimodality imaging study with this prerequisite in mind, recruiting HNSCC patients for dose painting in RT. A pilot study by Subesinghe *et al*[37] emphasized the importance of reproducing the positioning for assessing early RT treatment response.

^{18}F-FDG PET/CT and DW-MRI have been the focus of numerous studies in general HNSCC cohorts to determine correlation, if any, between SUV and ADC values, with variable results. SUV and ADC remain exploratory imaging metrics yet to be fully explored and understood in HPV-HNSCC patients. A study by Varoquax *et al*[38] involving 24 primary and 10 recurrent HNSCC showed no significant correlation between SUV values (SUV_{max}, SUV_{mean} or SUV_{min}) and ADC values (ADC_{max}, ADC_{mean} or ADC_{min}), nor did Choi *et al*[39] find significant correlation between SUV_{mean} and ADC_{mean} in 47 primary HNSCC. Rather, Nakajo *et al*[15] found significant negative correlation between SUV_{max} and ADC_{mean} in a study of 28 primary HNSCC tumors and Nakamatsu *et al*[26] demonstrated significant negative correlation in 41 neck nodal metastases between SUV values (SUV_{max}, SUV_{mean}) and ADC values (ADC_{mean}, ADC_{min}). In our study, similar results were obtained from a total of 11 neck nodal metastases and 5 primary HPV- HNSCC showing a significant strong negative correlation between the ADC_{mean} and SUV_{mean} pre-Tx ($\rho = -0.67$, $P = 0.01$). Further validation of the correlations with larger patient populations is needed, but was beyond the scope of this

study. Preda *et al*[40] concluded in a study with 57 HNSCC primary tumors that "the combination of SUV_{max} and ADC_{min} improves the prognostic role of the two separate parameters".

The present study showed an increase in $\Delta ADC\ Wk_{2-3}$ for the HPV- patient with NED in comparison with the DOD and AWD HPV- patients in both primary tumor and neck nodal metastases, in agreement with above-mentioned studies. Also, the pre-Tx ADC values of the primary tumor and neck nodal metastases for NED is lower than in the group of AWD and DOD, showing that lower pre-Tx ADC values are related to a good response to treatment and are consistent with the previous literature[9,41].

The % change in ΔADC for primary tumor and neck nodal metastases depict the different Tx responses, suggesting the possibility of identifying HPV- patients with poor prognosis at an early stage to individualize and adapt RT treatment (*i.e.*, through dose-escalation). Vandecaveye *et al*[42] showed in neck nodal metastases and primary tumors that ΔADC (Week 2 and Week 4 during CRT) was significantly lower ($P < 0.0001$) in lesions with recurrence than in lesions with a complete response.

Individualization of treatment is especially important in the subgroup of HPV- patients who were part of this study. A limitation of the study was that there were a relatively small number of HPV- patients as the recruitment was highly selective in Spain. However, we felt that this selectivity was justified given that these subtypes of HPV- patients are the ones who have poor prognoses in HNSCC[28]. The initial results need to be addressed through validation in future studies.

Our study offers insight on how to manage and understand valuable quantitative imaging biomarkers, such as SUV and ADC for HPV- HNSCC, with the objective of integrating them into the development of biological adaptive RT in the future.

These results are preliminary in nature and are indicative, and not definitive, trends rendered by the imaging metrics due to the small sample size of HPV- HNSCC patients in a Meixoeiro Hospital of Vigo Experience.

ACKNOWLEDGMENTS

COMMENTS

Background
Human papillomavirus (HPV) negative (-) head and neck squamous cell carcinoma (HNSCC) patients have poor outcomes compared with HPV-positive (HPV+) cancers. Individualization of radiotherapy is especially important in the subgroup of HPV- patients and imaging metrics derived from multimodality imaging can be critical for its implementation.

Research frontiers
In an effort to perform biologically guided adaptive radiotherapy, it is critical to understand how different functional imaging techniques interact and potentially complement each other.

Innovations and breakthroughs
Multimodality imaging in HPV- HNSCC suggests that tumor cell density is inversely proportional to glucose metabolism in a Meixoeiro Hospital of Vigo Experience. These results are promising and need to be validated in larger populations.

Applications
Diffusion-weighted magnetic resonance imaging and ^{18}F-labeled fluoro-deoxyglucose positron emission tomography/computed tomography are two valuable imaging techniques that may help build the framework for adaptive radiotherapy based on functional images in future clinical trials by investigating tumor cellularity and glucose metabolism before, during and after RT in HPV- HNSCC.

Terminology
^{18}F-FDG: Fluorine-18 fludeoxyglucose; ADC: Apparent diffusion coefficient; AWD: Alive with disease; DOC: Dead of other causes; DOD: Dead of disease; DW-MRI: Diffusion-weighted magnetic resonance imaging; HNC: Head and neck cancer; HNSCC: Head and neck squamous cell carcinoma; HPV-: Human papillomavirus negative; HPV+: Human papillomavirus positive; IMRT: Intensity modulated radiation therapy; MRI: Magnetic resonance imaging; NED: No evidence of disease; PET/CT: Positron emission tomography/computed tomography; ROI: Region of interest; RT: Radiotherapy.

Peer-review
This is a good paper.

REFERENCES

1   **Galceran**. Europa: Estimaciones de la incidencia y la supervivencia del cáncer en Espa-a y su situación en Europa, 2014

2   **Sanderson RJ**, Ironside JA. Squamous cell carcinomas of the head and neck. *BMJ* 2002; **325**: 822-827 [PMID: 12376446 DOI: 10.1136/bmj.325.7368.822]

3   **Seijas-Tamayo R**, Fernández-Mateos J, Adansa Klain JC, Mesía R, Pastor Borgoñón M, Pérez-Ruiz E, Vázquez Fernández S, Salvador Coloma C, Rueda Domínguez A, Taberna M, Martínez-Trufero J, Bonfill Abella T, Vázquez Estévez S, Pollán M, Del Barco Morillo E, Cruz-Hernández JJ. Epidemiological characteristics of a Spanish cohort of patients diagnosed with squamous cell carcinoma of head and neck: distribution of risk factors by tumor location. *Clin Transl Oncol* 2016; **18**: 1114-1122 [PMID: 27112939 DOI: 10.1007/s12094-016-1493-1]

4   **Fakhry C**, Westra WH, Li S, Cmelak A, Ridge JA, Pinto H, Forastiere A, Gillison ML. Improved survival of patients with human papillomavirus-positive head and neck squamous cell carcinoma in a prospective clinical trial. *J Natl Cancer Inst* 2008; **100**: 261-269 [PMID: 18270337 DOI: 10.1093/jnci/djn011]

5   **Jansen JF**, Schöder H, Lee NY, Stambuk HE, Wang Y, Fury MG, Patel SG, Pfister DG, Shah JP, Koutcher JA, Shukla-Dave A. Tumor metabolism and perfusion in head and neck squamous cell carcinoma:

pretreatment multimodality imaging with 1H magnetic resonance spectroscopy, dynamic contrast-enhanced MRI, and [18F]FDG-PET. *Int J Radiat Oncol Biol Phys* 2012; **82**: 299-307 [PMID: 21236594 DOI: 10.1016/j.ijrobp.2010.11.022]

6   **Padhani AR**, Liu G, Koh DM, Chenevert TL, Thoeny HC, Takahara T, Dzik-Jurasz A, Ross BD, Van Cauteren M, Collins D, Hammoud DA, Rustin GJ, Taouli B, Choyke PL. Diffusion-weighted magnetic resonance imaging as a cancer biomarker: consensus and recommendations. *Neoplasia* 2009; **11**: 102-125 [PMID: 19186405 DOI: 10.1593/neo.81328]

7   **Chenevert TL**, Stegman LD, Taylor JM, Robertson PL, Greenberg HS, Rehemtulla A, Ross BD. Diffusion magnetic resonance imaging: an early surrogate marker of therapeutic efficacy in brain tumors. *J Natl Cancer Inst* 2000; **92**: 2029-2036 [PMID: 11121466 DOI: 10.1093/jnci/92.24.2029]

8   **Ng SH**, Liao CT, Lin CY, Chan SC, Lin YC, Yen TC, Chang JT, Ko SF, Fan KH, Wang HM, Yang LY, Wang JJ. Dynamic contrast-enhanced MRI, diffusion-weighted MRI and (18)F-FDG PET/CT for the prediction of survival in oropharyngeal or hypopharyngeal squamous cell carcinoma treated with chemoradiation. *Eur Radiol* 2016; **26**: 4162-4172 [PMID: 26911889 DOI: 10.1007/s00330-016-4276-8]

9   **Kim S**, Loevner L, Quon H, Sherman E, Weinstein G, Kilger A, Poptani H. Diffusion-weighted magnetic resonance imaging for predicting and detecting early response to chemoradiation therapy of squamous cell carcinomas of the head and neck. *Clin Cancer Res* 2009; **15**: 986-994 [PMID: 19188170 DOI: 10.1158/1078-0432.CCR-08-1287]

10 **Vandecaveye V**, Dirix P, De Keyzer F, Op de Beeck K, Vander Poorten V, Hauben E, Lambrecht M, Nuyts S, Hermans R. Diffusion-weighted magnetic resonance imaging early after chemoradiotherapy to monitor treatment response in head-and-neck squamous cell carcinoma. *Int J Radiat Oncol Biol Phys* 2012; **82**: 1098-1107 [PMID: 21514067 DOI: 10.1016/j.ijrobp.2011.02.044]

11 **Schöder H**, Fury M, Lee N, Kraus D. PET monitoring of therapy response in head and neck squamous cell carcinoma. *J Nucl Med* 2009; **50** Suppl 1: 74S-88S [PMID: 19380408 DOI: 10.2967/jnumed.108.057208]

12 **Ong SC**, Schöder H, Lee NY, Patel SG, Carlson D, Fury M, Pfister DG, Shah JP, Larson SM, Kraus DH. Clinical utility of 18F-FDG PET/CT in assessing the neck after concurrent chemoradiotherapy for Locoregional advanced head and neck cancer. *J Nucl Med* 2008; **49**: 532-540 [PMID: 18344440 DOI: 10.2967/jnumed.107.044792]

13 **Wong RJ**, Lin DT, Schöder H, Patel SG, Gonen M, Wolden S, Pfister DG, Shah JP, Larson SM, Kraus DH. Diagnostic and prognostic value of [(18)F]fluorodeoxyglucose positron emission tomography for recurrent head and neck squamous cell carcinoma. *J Clin Oncol* 2002; **20**: 4199-4208 [PMID: 12377963 DOI: 10.1200/JCO.2002.02.590]

14 **Schwartz DL**, Rajendran J, Yueh B, Coltrera MD, Leblanc M, Eary J, Krohn K. FDG-PET prediction of head and neck squamous cell cancer outcomes. *Arch Otolaryngol Head Neck Surg* 2004; **130**: 1361-1367 [PMID: 15611393 DOI: 10.1001/archotol.130.12.1361]

15 **Nakajo M**, Nakajo M, Kajiya Y, Tani A, Kamiyama T, Yonekura R, Fukukura Y, Matsuzaki T, Nishimoto K, Nomoto M, Koriyama C. FDG PET/CT and diffusion-weighted imaging of head and neck squamous cell carcinoma: comparison of prognostic significance between primary tumor standardized uptake value and apparent diffusion coefficient. *Clin Nucl Med* 2012; **37**: 475-480 [PMID: 22475897 DOI: 10.1097/RLU.0b013e318248524a]

16 **Min M**, Lee MT, Lin P, Holloway L, Wijesekera Dj, Gooneratne D, Rai R, Xuan W, Fowler A, Forstner D, Liney G. Assessment of serial multi-parametric functional MRI (diffusion-weighted imaging and R2*) with (18)F-FDG-PET in patients with head and neck cancer treated with radiation therapy. *Br J Radiol* 2016; **89**: 20150530 [PMID: 26648404 DOI: 10.1259/bjr.20150530]

17 **Goodyear MD**, Krleza-Jeric K, Lemmens T. The Declaration of Helsinki. *BMJ* 2007; **335**: 624-625 [PMID: 17901471 DOI: 10.1136/bmj.39339.610000.BE]

18 **Bockmühl U**, Ishwad CS, Ferrell RE, Gollin SM. Association of 8p23 deletions with poor survival in head and neck cancer.

Otolaryngol Head Neck Surg 2001; **124**: 451-455 [PMID: 11283506 DOI: 10.1067/mhn.2001.114794]

19 **Landesa-Vazquez I**, Alba-Castro JL, Mera-Iglesias M, Aramburu-Nunez D, Lopez-Medina A, Munoz-Garzon V. ARTFIBio: A Cross-Platform Image Registration Tool for Tumor Response Quantification in Head and Neck Cancer. *Ieee-Embs International Conference on Biomedical and Health Informatics* (Bhi) 2014: 149-152 [DOI: 10.1109/BHI.2014.6864326]

20 **Mattes D**, Haynor DR, Vesselle H, Lewellen TK, Eubank W. Nonrigid multimodality image registration. *P Soc Photo-Opt Ins* 2001; **2**: 1609-1620 [DOI: 10.1117/12.431046]

21 **Stejskal EO**, Tanner JE. Spin Diffusion Measurements: Spin Echoes in the Presence of a Time-Dependent Field Gradient. *J Chem Phys* 1965; **42**: 288-292 [DOI: 10.1063/1.1695690]

22 **IAEA**. Quantitative Nuclear Medicine Imaging: Concepts, Requirements and Methods. Austria: IAEA Library, 2014

23 **Cohen J**. The statistical power of abnormal-social psychological research: a review. *J Abnorm Soc Psychol* 1962; **65**: 145-153 [PMID: 13880271 DOI: 10.1037/h0045186]

24 **R Project**. GNU Operating System. Available from: URL: http://www.gnu.org/licenses/gpl.html

25 **Gawlitza M**, Purz S, Kubiessa K, Boehm A, Barthel H, Kluge R, Kahn T, Sabri O, Stumpp P. In Vivo Correlation of Glucose Metabolism, Cell Density and Microcirculatory Parameters in Patients with Head and Neck Cancer: Initial Results Using Simultaneous PET/MRI. *PLoS One* 2015; **10**: e0134749 [PMID: 26270054 DOI: 10.1371/journal.pone.0134749]

26 **Nakamatsu S**, Matsusue E, Miyoshi H, Kakite S, Kaminou T, Ogawa T. Correlation of apparent diffusion coefficients measured by diffusion-weighted MR imaging and standardized uptake values from FDG PET/CT in metastatic neck lymph nodes of head and neck squamous cell carcinomas. *Clin Imaging* 2012; **36**: 90-97 [PMID: 22370129 DOI: 10.1016/j.clinimag.2011.05.002]

27 **Jemal A**, Siegel R, Xu J, Ward E. Cancer statistics, 2010. *CA Cancer J Clin* 2010; **60**: 277-300 [PMID: 20610543 DOI: 10.3322/caac.20073]

28 **Ang KK**, Harris J, Wheeler R, Weber R, Rosenthal DI, Nguyen-Tân PF, Westra WH, Chung CH, Jordan RC, Lu C, Kim H, Axelrod R, Silverman CC, Redmond KP, Gillison ML. Human papillomavirus and survival of patients with oropharyngeal cancer. *N Engl J Med* 2010; **363**: 24-35 [PMID: 20530316 DOI: 10.1056/NEJMoa0912217]

29 **Abdel Razek AA**, Kamal E. Nasopharyngeal carcinoma: correlation of apparent diffusion coefficient value with prognostic parameters. *La Radiologia medica* 2013; **118**: 534-539 [PMID: 23090251 DOI: 10.1007/s11547-012-0890-x]

30 **Abdel Razek AA**, Kandeel AY, Soliman N, El-shenshawy HM, Kamel Y, Nada N, Denewar A. Role of diffusion-weighted echo-planar MR imaging in differentiation of residual or recurrent head and neck tumors and posttreatment changes. *AJNR American journal of neuroradiology* 2007; **28**: 1146-1152 [PMID: 17569975 DOI: 10.3174/ajnr.A0491]

31 **Razek AA**, Nada N. Correlation of Choline/Creatine and Apparent Diffusion Coefficient values with the prognostic parameters of Head and Neck Squamous Cell Carcinoma. *NMR in biomedicine* 2016; **29**: 483-489 [PMID: 26867020 DOI: 10.1002/nbm.3472]

32 **Han M**, Kim SY, Lee SJ, Choi JW. The Correlations Between MRI Perfusion, Diffusion Parameters, and 18F-FDG PET Metabolic Parameters in Primary Head-and-Neck Cancer: A Cross-Sectional Analysis in Single Institute. *Medicine* (Baltimore) 2015; **94**: e2141 [PMID: 26632740 DOI: 10.1097/MD.0000000000002141]

33 **Shukla-Dave A**, Lee NY, Jansen JF, Thaler HT, Stambuk HE, Fury MG, Patel SG, Moreira AL, Sherman E, Karimi S, Wang Y, Kraus D, Shah JP, Pfister DG, Koutcher JA. Dynamic contrast-enhanced magnetic resonance imaging as a predictor of outcome in head-and-neck squamous cell carcinoma patients with nodal metastases. Int *J Radiat Oncol Biol Phys* 2012; **82**: 1837-1844 [PMID: 21601373 DOI: 10.1016/j.ijrobp.2011.03.006]

34 **van der Heide UA**, Houweling AC, Groenendaal G, Beets-Tan RG, Lambin P. Functional MRI for radiotherapy dose painting. *Magn Reson Imaging* 2012; **30**: 1216-1223 [PMID: 22770686 DOI:

10.1016/j.mri.2012.04.010]

35   **Thorwarth D**, Beyer T, Boellaard R, de Ruysscher D, Grgic A, Lee JA, Pietrzyk U, Sattler B, Schaefer A, van Elmpt W, Vogel W, Oyen WJ, Nestle U. Integration of FDG-PET/CT into external beam radiation therapy planning: technical aspects and recommendations on methodological approaches. *Nuklearmedizin* 2012; **51**: 140-153 [PMID: 22473130 DOI: 10.3413/Nukmed-0455-11-12]

36   **Dirix P**, Vandecaveye V, De Keyzer F, Stroobants S, Hermans R, Nuyts S. Dose painting in radiotherapy for head and neck squamous cell carcinoma: value of repeated functional imaging with (18)F-FDG PET, (18)F-fluoromisonidazole PET, diffusion-weighted MRI, and dynamic contrast-enhanced MRI. *J Nucl Med* 2009; **50**: 1020-1027 [PMID: 19525447 DOI: 10.2967/jnumed.109.062638]

37   **Subesinghe M**, Scarsbrook AF, Sourbron S, Wilson DJ, McDermott G, Speight R, Roberts N, Carey B, Forrester R, Gopal SV, Sykes JR, Prestwich RJ. Alterations in anatomic and functional imaging parameters with repeated FDG PET-CT and MRI during radiotherapy for head and neck cancer: a pilot study. *BMC Cancer* 2015; **15**: 137 [PMID: 25885109 DOI: 10.1186/s12885-015-1154-8]

38   **Varoquaux A**, Rager O, Lovblad KO, Masterson K, Dulguerov P, Ratib O, Becker CD, Becker M. Functional imaging of head and neck squamous cell carcinoma with diffusion-weighted MRI and FDG PET/CT: quantitative analysis of ADC and SUV. *Eur J Nucl Med Mol Imaging* 2013; **40**: 842-852 [PMID: 23436068 DOI: 10.1007/s00259-013-2351-9]

39   **Choi SH**, Paeng JC, Sohn CH, Pagsisihan JR, Kim YJ, Kim KG, Jang JY, Yun TJ, Kim JH, Han MH, Chang KH. Correlation of 18F-FDG uptake with apparent diffusion coefficient ratio measured on standard and high b value diffusion MRI in head and neck cancer. *J Nucl Med* 2011; **52**: 1056-1062 [PMID: 21680692 DOI: 10.2967/jnumed.111.089334]

40   **Preda L**, Conte G, Bonello L, Giannitto C, Travaini LL, Raimondi S, Summers PE, Mohssen A, Alterio D, Cossu Rocca M, Grana C, Ruju F, Bellomi M. Combining standardized uptake value of FDG-PET and apparent diffusion coefficient of DW-MRI improves risk stratification in head and neck squamous cell carcinoma. *Eur Radiol* 2016 [PMID: 26965504 DOI: 10.1007/s00330-016-4284-8]

41   **Hatakenaka M**, Nakamura K, Yabuuchi H, Shioyama Y, Matsuo Y, Kamitani T, Yonezawa M, Yoshiura T, Nakashima T, Mori M, Honda H. Apparent diffusion coefficient is a prognostic factor of head and neck squamous cell carcinoma treated with radiotherapy. *Jpn J Radiol* 2014; **32**: 80-89 [PMID: 24408077 DOI: 10.1007/s11604-013-0272-y]

42   **Vandecaveye V**, Dirix P, De Keyzer F, de Beeck KO, Vander Poorten V, Roebben I, Nuyts S, Hermans R. Predictive value of diffusion-weighted magnetic resonance imaging during chemoradiotherapy for head and neck squamous cell carcinoma. *Eur Radiol* 2010; **20**: 1703-1714 [PMID: 20179939 DOI: 10.1007/s00330-010-1734-6]

Baishideng®

Published by **Baishideng Publishing Group Inc**
8226 Regency Drive, Pleasanton, CA 94588, USA
Telephone: +1-925-223-8242
Fax: +1-925-223-8243
E-mail: bpgoffice@wjgnet.com
Help Desk: http://www.wjgnet.com/esps/helpdesk.aspx
http://www.wjgnet.com